Electronic Supplementary Information

Immune remodeling triggered by photothermal therapy with semiconducting polymer nanoparticles in combination with chemotherapy to inhibit metastatic cancers

Yuming Yang,[a‡] Minjie Xu,[b‡] Zhe Wang,[b] Yanqing Yang,[a] Jie Liu,[*a] Qinglian Hu,[*b] Lin Li[*a] and Wei Huang[*ac]

[a] Key Laboratory of Flexible Electronics (KLOFE) Institute of Advanced Materials (IAM), Nanjing Tech University, Nanjing 211800, China. E-mail: iamjieliu@njtech.edu.cn; iamlli@njtech.edu.cn

[b] College of Biotechnology and Bioengineering, Zhejiang University of Technology, Hangzhou 310032, China. E-mail: huqinglian@zjut.edu.cn

[c] Frontiers Science Center for Flexible Electronics (FSCFE), Shaanxi Institute of Flexible Electronics (SIFE) & Shaanxi Institute of Biomedical Materials and Engineering (SIBME), Northwestern Polytechnical University (NPU), 127 West Youyi Road, Xi'an 710072, China. E-mail: iamwhuang@nwpu.edu.cn

Materials

2,5-Bis(trimethylstannyl)selenophene and 3,6-bis(5-bromothiophen-2-yl)-2,5-bis(2-decyltetradecyl)-2,5-dihydropyrrolo[3,4-*c*]pyrrole-1,4-dione and were purchased from Derthon Optoelectronic Materials Science Technology Co LTD. 1,2-Distearoyl-*sn*-glycero-3-phosphoetanolamine-*N*-[methoxy(polyethyleneglycol)-2000] (DSPE-

PEG_{2000}) was purchased from Laysan Bio, Inc. Anti-CD3-PerCP-Cy5.5 (catalog number 100327), anti-CD4-FITC (catalog number 100509), and anti-CD8-PE (catalog number 100707), anti-CD25-PE (catalog number 101903), anti-CD11b-PE (catalog number 101207) and anti-mouse Ly-6G/Ly-6C (Gr-1) -FITC (catalog number 108405) antibodies were purchased from Biolegend. Mini-Q water (18.2 MΩ) was obtained by a Milli-Q Plus System (Millipore Corporation, Bedford, USA) and used for all experiments requiring aqueous medium. Phosphate buffer saline (PBS) and dulbecco's modified eagle medium (DMEM) were obtained from Aladdin Reagent Co., Ltd. (China). All other chemicals were purchased from Sigma-Aldrich or Energy Chemical (China).

Characterization

Nuclear Magnetic Resonance (NMR) spectra were recorded on a JNM-ECZ400S/L1 400 MHz spectrometer. UV-vis-NIR spectra were collected on Shimadzu UV-1750 spectrometer. Photoluminescence (PL) spectra were recorded on a fluorescence spectrophotometer F-4600, or an Edinburgh instruments FLS980 apparatus equipped with a Xe lamp as excitation source and a liquid nitrogen-cooled InGaAs detector. Fluorescence lifetime were recorded on an Edinburgh instruments FLS980 apparatus. Gel Permeation Chromatography (GPC) spectra were measured on a Breeze system. Dynamic light scattering (DLS) measurements were performed on a Micromeritics Nanoplus-3 apparatus (US). Transmission electron microscopy (TEM) images were recorded on a JEOL JEM-1400Plus electron microscope with an accelerating voltage of 120 kV.

Synthesis

2,5-bis(2-decyltetradecyl)-3,6-bis(5-(selenophen-2-yl)thiophen-2-yl)-2,5-dihydropyrrolo[3,4-c]pyrrole-1,4-dione (DPSe): 3,6-Bis(5-bromothiophen-2-yl)-2,5-bis(2-decyltetradecyl)-2,5-dihydropyrrolo[3,4-*c*]pyrrole-1,4-dione (113 mg, 0.1 mmol), tributyl(selenophen-2-yl)stannane (126 mg, 0.3 mmol), $Pd_2(dba)_3$ (3 mg, 3.3 μmol), P(*o*-tolyl)$_3$ (3 mg, 9.8 μmol) and toluene (10 mL) were added into a Schlenk tube under argon atmosphere. The reaction mixture was heated at 100 ℃ for 24 h. Then the solvent was removed under reduced pressure. The residue was purified by silica gel column chromatography (petroleum ether /dichloromethane =2/3), yielding DPSe as a purple solid (100 mg, yield: 81%). ^{1}H NMR (400 MHz, $CDCl_3$) δ (ppm): 8.91−8.90 (d, *J* = 4 Hz, 2H), 8.01−8.00 (d, *J* = 4 Hz, 2H), 7.48−7.47 (d, *J* = 4 Hz, 2H), 7.31−7.29 (t, *J* = 8 Hz, 2H), 7.26−7.25 (d, *J* = 4 Hz, 2H), 4.04−4.03 (d, *J* = 4 Hz, 2H), 2.02−1.95 (m, 2H), 1.33−1.21 (m, 80H), 0.86−0.85 (m, 12H). ^{13}C NMR (100 MHz, $CDCl_3$) δ: 161.6, 144.84, 141.08, 139.44, 136.68, 131.66, 130.62, 128.24, 127.26, 125.42, 108.36, 46.25, 37.91, 31.92, 31.29, 30.06, 29.71, 29.67, 29.66, 29.65, 29.62, 29.37, 26.33, 22.69, 14.13.

2,5-Bis(2-decyltetradecyl)-3-(5-(5-methylselenophen-2-yl)thiophen-2-yl)-6-(5-methylthiophen-2-yl)-2,5-dihydropyrrolo[3,4-c]pyrrole-1,4-dione (PDPSe) : 3,6-Bis(5-bromothiophen-2-yl)-2,5-bis(2-decyltetradecyl)-2,5-dihydropyrrolo[3,4-*c*]pyrrole-1,4-dione (113 mg, 0.1 mmol), 2,5-bis(trimethylstannyl)selenophene (45.6 mg, 0.1 mmol), $Pd_2(dba)_3$ (3 mg, 3.3 μmol), P(*o*-tolyl)$_3$ (3 mg, 9.8 μmol) and toluene (10 mL) were added into a Schlenk tube. The reaction mixture was heated at 100 ℃ for

2 h under argon atmosphere. The mixture was dropped slowly into methanol (150 mL) to precipitate the crude polymer followed by filtration. Then the crude polymer was dissolved in dichloromethane (200 mL), washed with water (100 mL × 3) and dried over $MgSO_4$. After filtration with filter paper, the solution was concentrated to ~10 mL and dropped into methanol. The precipitated PDPSe (70 mg, yield: 62%) was collected as a green solid. ^{1}H NMR (400 MHz, $CDCl_3$) δ (ppm): 9.07−8.97 (br), 7.22−6.96 (br), 2.24−2.20 (br), 2.03−1.97 (br), 1.25−1.21(br), 0.86−0.85 (br).

Preparation of nanoparticles

The nanoparticles were synthesized using a nanoprecipitation method. For the synthesis of PDPSe NPs, PDPSe (1 mg) and DSPE-PEG_{2000} (2 mg) were dissolved in tetrahydrofuran (THF, 2 mL) and stirred for 24 h at room temperature. The solution was added to Milli-Q water (10 mL), which was sonicated for 2 min by a probe sonicator. The THF solvent was removed by stirring the solution in fume hood at room temperature. After filtration through a 0.22 micron filter, PDPSe NPs were obtained and concentrated by ultrafilter for further use. DPSe NPs were prepared in a similar procedure.

Stability of nanoparticles

To evaluate the colloidal stability of nanoparticles, the size of nanoparticles in PBS (pH = 7.4) were tested over 14 days by DLS. To study the photostability of nanoparticles, NPs were irradiated by a 635 nm laser (1.5 W cm^{-2}) for 0.5 h. The absorption spectra were measured at different time points.

Calculation of the photothermal conversion efficiency (PCE)

According to previous report,[1] the PCE of NPs was calculated from Equation (1)

$$\eta = \frac{hS(T_{max} - T_{surr}) - Q_{dis}}{I(1 - 10^{-A})} \qquad (1)$$

where h is the heat transfer coefficient, S is the surface area of the container, T_{max} is the maximum steady-state temperature of NP solution, T_{surr} is the ambient temperature of environment, Q_{dis} is the heat dissipation from the light absorbed by the solvent and the container, I is the incident laser power, and A is the absorbance of the NPs at the incident light wavelength (808 nm for PDPSe NPs and 635 nm for DPSe NPs). The value of hS was obtained from Equation (2)

$$\tau_s = \frac{m_D c_D}{hS} \qquad (2)$$

where τ_s represents the time constant for heat transfer of the system, which was determined to from Fig. S10 for DPSe NPs and Fig. S11 for PDPSe NPs; m_D (0.3 g) and c_D (4.2 J g^{-1} $^oC^{-1}$) represent the mass and heat capacity, respectively, of the pure water used to disperse the NPs. Q_{dis} was calculated from Equation (3)

$$Q_{dis} = \frac{m_D c_D (T_{max(water)} - T_{surr})}{\tau_{s(water)}} \qquad (3)$$

where $T_{max(water)}$ is the maximum steady-state temperature of the pure water, and $\tau_{s(water)}$ is the time constant for heat transfer of the pure water. According to the obtained data and Equations (1-3), the PCE of NPs can be determined.

Cell Lines and Animals

Mouse breast cancer (4T1) cell lines were cultured in RPMI-1640 medium at 37 ℃ in an incubator with 5% CO_2 concentration. RPMI-1640 media contained 10% fetal bovine serum (FBS) and 1% Penicillin-Streptomycin Solution.

Female BALB/c mice (4 weeks old) were obtained from the Shanghai SLAC Laboratory Animal (Shanghai, China). All animal experiments were approved by the Institutional Ethical Committee of Animal Experimentation of Zhejiang University of Technology.

***In vitro* cytotoxicity**

Conventional MTT assay was used to evaluate the cytotoxicity of PDPSe NPs and TPZ.

The viability of 4T1 cells treated with different concentrations of PDPSe NPs was evaluated. 4T1 cells were seeded on 96-well plates at a density of 10000 cells $well^{-1}$ and incubated 12 h. Then the medium was replaced with different concentrations of PDPSe NPs and cultivated 24 h. Each group was treated with or without 808 nm laser with power of 1.0 Wcm^{-2} for 5 min. After incubating with fresh RPMI-1640 medium for 24 h, MTT solutions were added into each well and cultivated at 37 ℃ for another 4 h. Finally, MTT solutions were replaced with 150 μL dimethyl sulfoxide (DMSO) formazan absorbance was determined by the microplate reader (ThemoMultiscan MK3, USA) at 490 nm. The cell viability of untreated group was set as 100%.

The viability of 4T1 cells treated with different concentrations of TPZ was evaluated. 4T1 cells were seeded on 96-well plates at a density of 10000 cells $well^{-1}$ and incubated 12 h. Then the medium was replaced with different concentrations of TPZ and cultivated 24 h. After incubating with fresh RPMI-1640 medium for 24 h, MTT solutions were added into each well and cultivated at 37 ℃ for another 4 h. Finally, MTT solutions were replaced with 150 μL dimethyl sulfoxide (DMSO) formazan

absorbance was determined by the microplate reader (ThemoMultiscan MK3, USA) at 490 nm. The cell viability of untreated group was set as 100%.

The viability of 4T1 cells treated with different concentrations of PDPSe NPs and TPZ was evaluated. 4T1 cells were seeded on 96-well plates at a density of 10000 cells $well^{-1}$ and incubated 12 h. Then the medium was replaced with different concentrations of PDPSe NPs and TPZ, and cultivated 24 h. Every group were treated with or without 808nm laser with power of 1.0 W cm^{-2} for 5 min. After incubating with fresh RPMI-1640 medium for 24 h, MTT solutions were added into each well and cultivated at 37 ℃ for another 4 h. Finally, MTT solutions were replaced with 150 μL dimethyl sulfoxide (DMSO) formazan absorbance was determined by the microplate reader (ThemoMultiscan MK3, USA) at 490 nm. The cell viability of untreated group was set as 100%.

Establishment of the 4T1 Bilateral Tumor Models

To establish the 4T1 bilateral tumor model, 4T1 cells (2×10^6) in 0.1 mL of PBS were injected subcutaneously on the right flank of female BALB/c mice of weight 20 g at day 0 (primary tumors) and injected subcutaneously on the left flank at day 6 (distant tumors).

***In vivo* Antitumor Effect Study**

Then the mice were randomly divided into six groups when the right flank tumor reach 100 mm^3 at day 9 (PBS, PDPSe NPs, TPZ, PBS + laser, PDPSe NPs + laser, and PDPSe NPs + laser + TPZ). TPZ was intravenously injected into mice via tail vein, and other therapeutic agents were injected into primary tumors at day 10 *via* intratumoral

injection. Then, the primary tumors that required PTT were exposed to an 808 nm laser irradiation for 10 min with a power density of 1.5 W cm^{-2}. The temperature changes of primary tumors treated with PTT were measured using an IR thermal camera (FOTRIC 220 s) and recorded at different irradiation time points. Tumor sizes were measured using vernier calipers and calculated every other day (tumor volume was calculated as $0.5 \times length \times width^2$).

Histology Study

In order to evaluate the antitumor efficiency, all the mice were sacrificed on day 24, and their tumor were harvested, weighted, washed by PBS and fixed in 4% paraformaldehyde for 24 h, and cut into 5 μm slices. The fixed slices were stained with Hematoxylin and eosin (H&E). Terminal transferased UTP nick-end labeling (TUNEL) assays was further used for conforming apoptosis of tumor after treatment. The major organs (heart, kidney, lung, spleen, liver) were also collected, weighted, washed and placed in 4% paraformaldehyde and stained with H&E.

Immunofluorescence Stain

After different treatments *in vivo*, the mice were sacrificed on day 24, the slices of primary tumors were blocked and incubated with primary antibodies of CD8+, CD206 and HIF-α, followed by the incubation with a secondary antibody and the nuclei were stained with Hoechst. Finally, the slices were visualized using a confocal laser scanning microscopy.

Serum Biochemistry Assay

To confirm the biosafety of PDPSe NPs in mice, all the mice were sacrificed on day

24. At the same time, mice blood was collected and centrifuged, and the supernatant was taken as the serum. Finally, each mice serum was characterized with an automated hematology analyzer.

Flow cytometry and ELISA assay

To evaluate the immune response induced by different treatments. The spleens of mice were harvested at day 2, 14, 17 and 24. Then single cell suspension of splenocytes was prepared using a 70 μm cell sieve and cultured 3 days.

Enzyme-linked immunosorbent assay (ELISA) was used to evaluate the cytokines(IFN-γ, TNF-α, IL-4) of supernatant of splenocytes after 3 days of culture. According to the manufacturer's protocols, the cytokines content of samples was calculated by comparing the OD of the samples to the standard curve.

The collected splenocytes were incubated with anti-CD3-PerCP-Cy5.5, anti-CD4-FITC, and anti-CD8-PE antibodies according to the standard protocols, and the content of CD4+ or CD8+ T cells were measured using a flow cytometry. The splenocytes incubated with anti-CD4-FITC and anti-CD25-PE antibodies according to the standard protocols and the Tregs was examined using a flow cytometry. The splenocytes incubated with anti-CD11b-PE and anti-Gr-1-FITC antibodies according to the standard protocols and the myeloid-derived suppressor cells (MDSC) was examined using a flow cytometry.

Statistical analysis

All data were presented as means±SEM. Two groups were performed with the Student's t-test. Statistical analyses between multiple groups were used one-way

analysis of variance. Statistical significance is denoted by **p<0.01 or *p<0.05.

Reference

1 J. Zhang, C. Yang, R. Zhang, R. Chen, Z. Zhang, W. Zhang, S. H. Peng, X. Chen, G. Liu, C. S. Hsu and C. S. Lee, *Adv. Funct. Mater.*, 2017, **27**, 1605094.

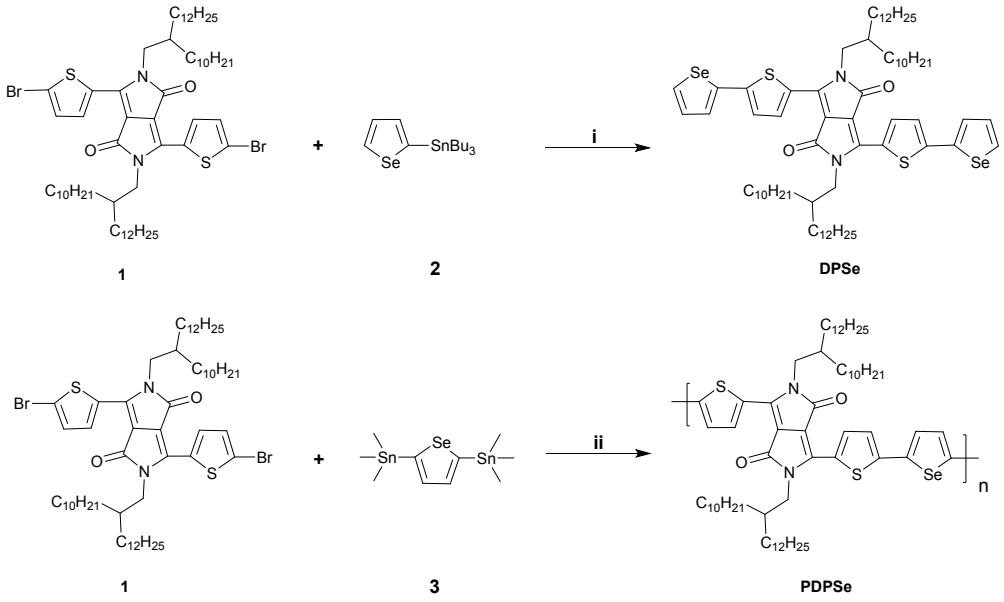

Scheme S1 Synthetic route to DPSe and PDPSe. Reagents and conditions: i) $Pd_2(dba)_3$, P(*o*-tolyl)$_3$, toluene, 100 °C, 24 h; ii) $Pd_2(dba)_3$, P(*o*-tolyl)$_3$, toluene, 100 °C, 2 h.

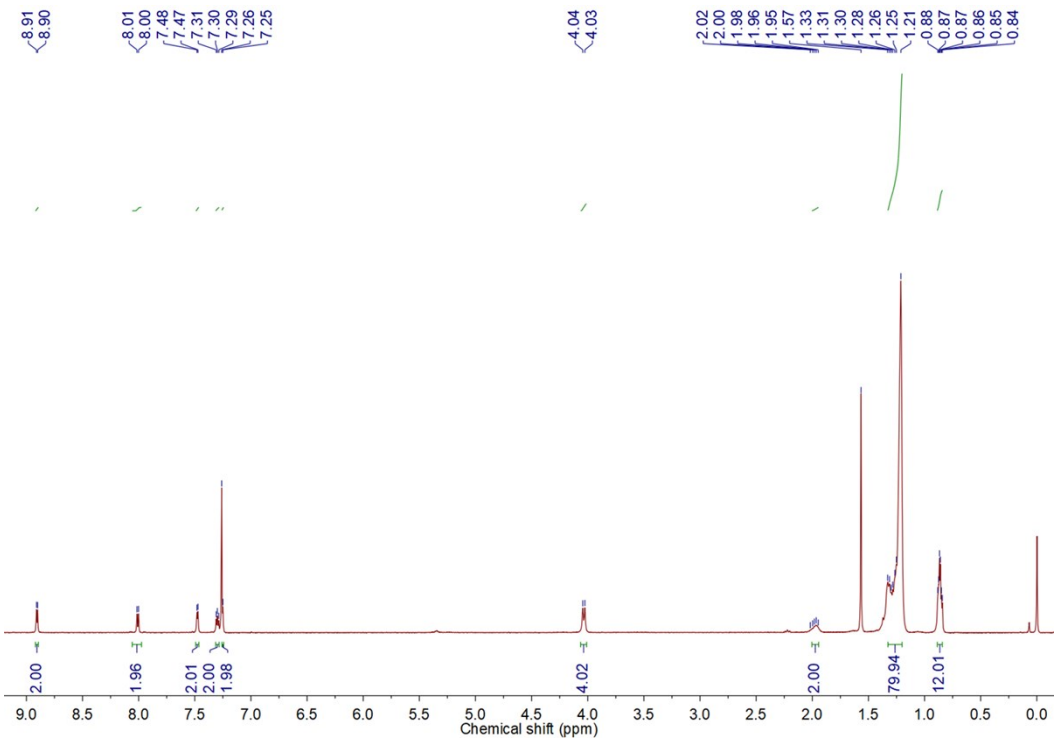

Fig. S1 ^{1}H NMR spectrum of DPSe in $CDCl_3$.

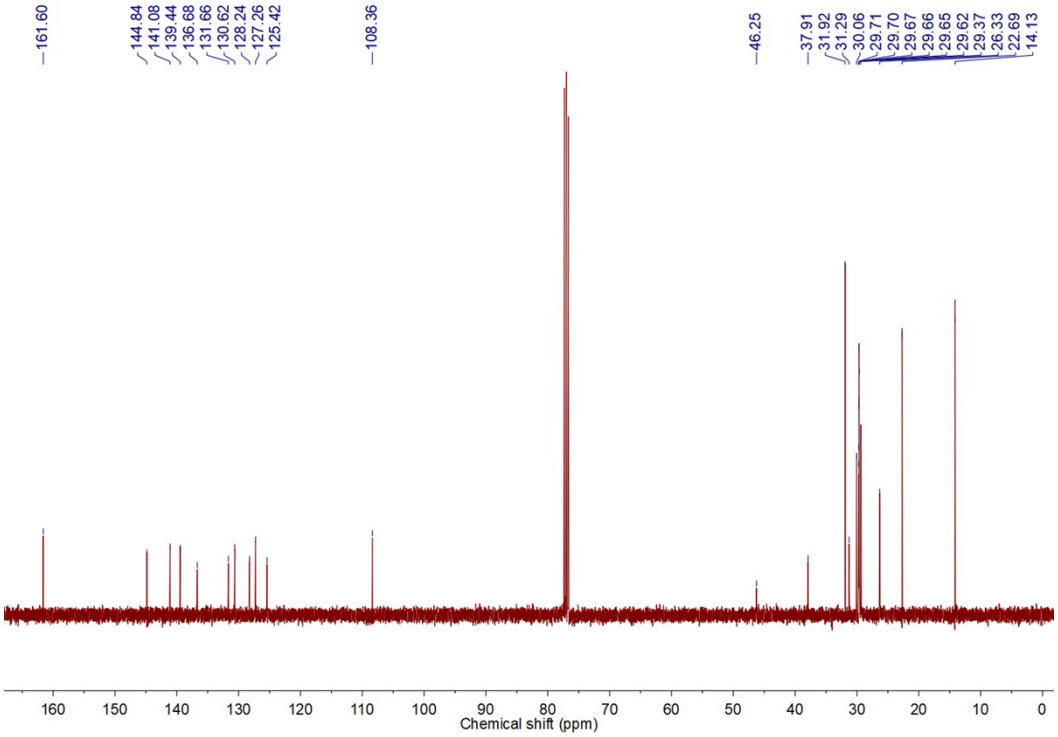

Fig. S2 ^{13}C NMR spectrum of DPSe in $CDCl_3$.

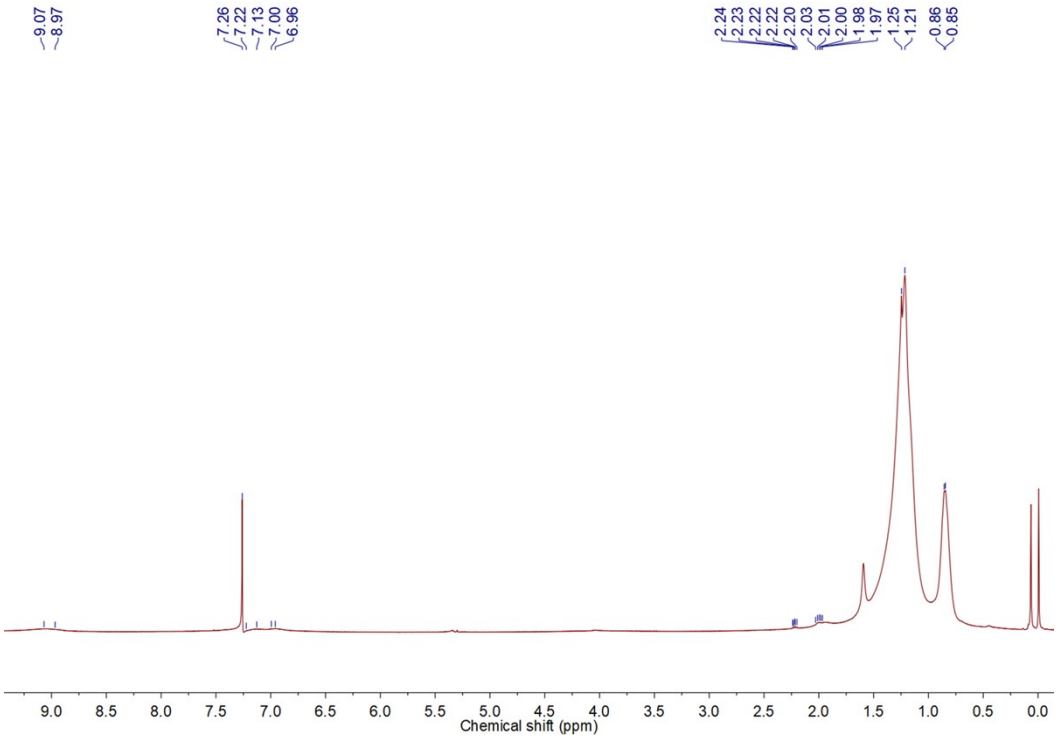

Fig. S3 ^{1}H NMR spectrum of PDPSe in $CDCl_3$.

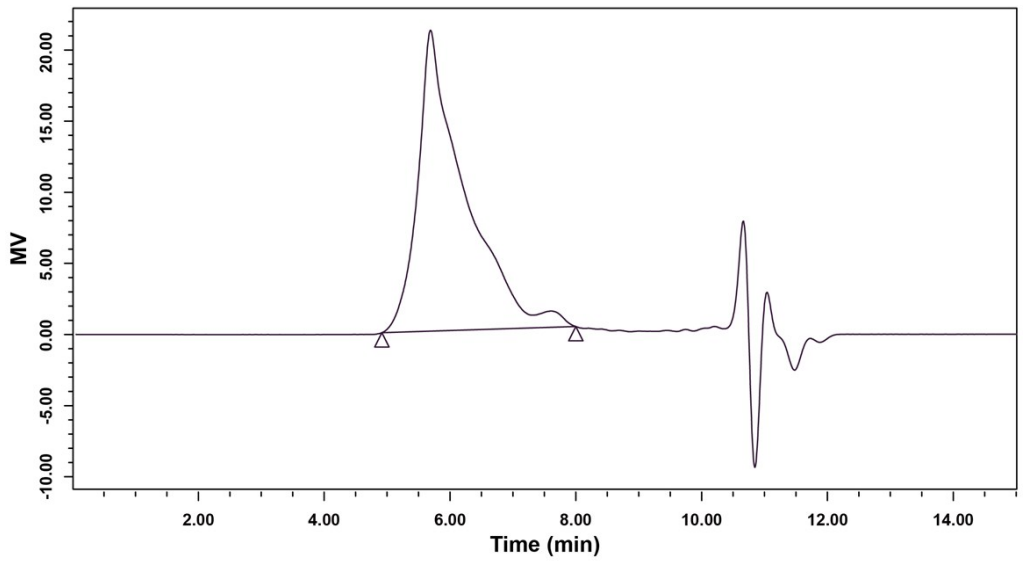

Fig. S4 GPC measurement of PDPSe, using THF as eluent and polystyrene as a standard. M_n: 72800 g mol^{-1}, PDI: 1.63.

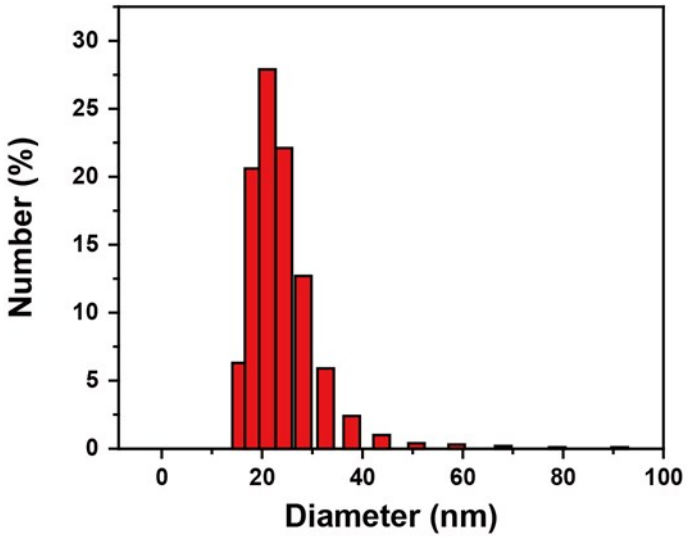

Fig. S DLS measurement of DPSe NPs in water.

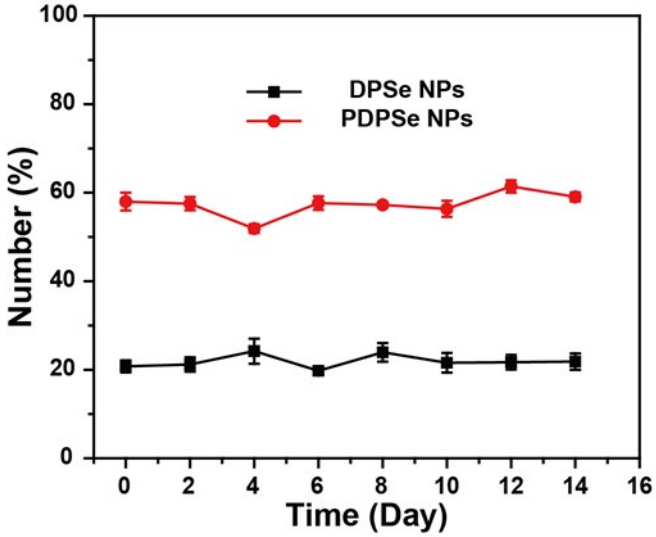

Fig. S6 DLS measurements of DPSe NPs and PDPSe NPs in 1 × PBS (pH = 7.4) over 14 days. Bars show means ± standard deviation (n = 3).

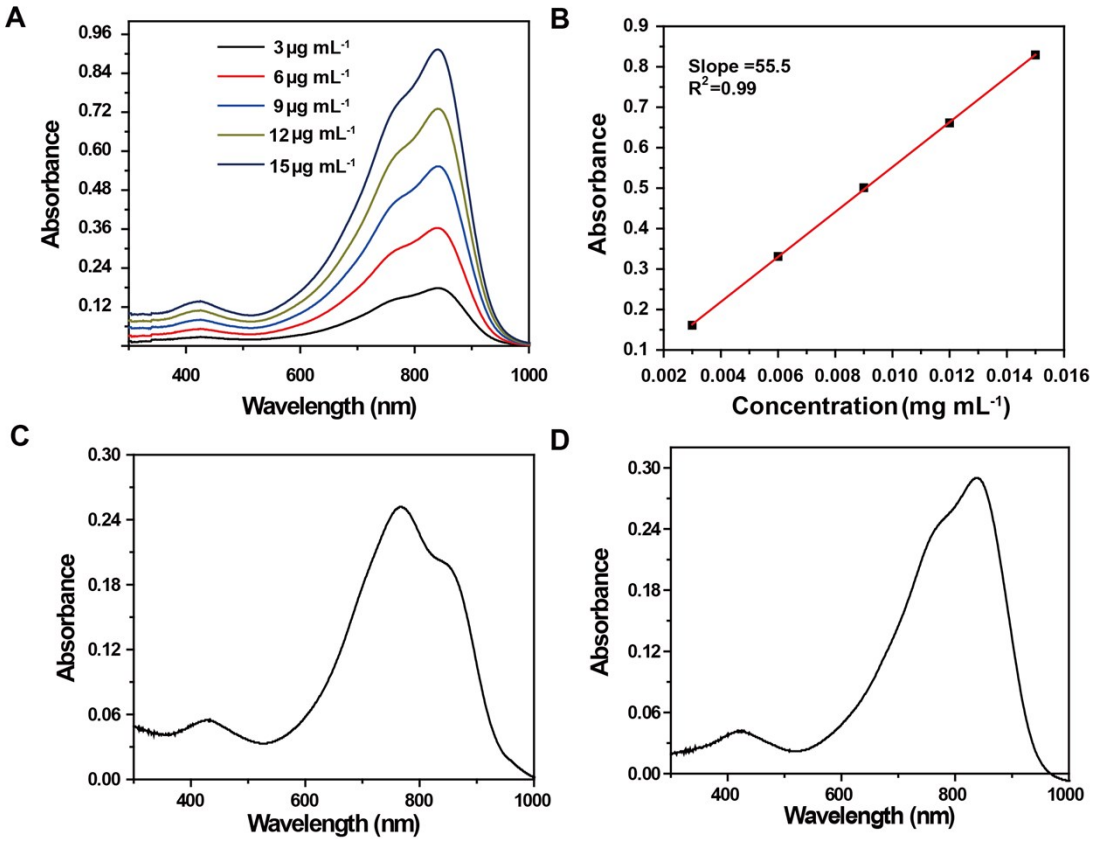

Fig. S7 Measurement of the mass extinction coefficient of PDPSe NPs in water. (A) Absorption spectra of PDPSe in chloroform with different concentrations. (B) Optical density of PDPSe at 808 nm plotted as a function of concentration of PDPSe in chloroform. The slope was used to determine the mass extinction coefficient (55.5 L g^{-1} cm^{-1}). (C) Absorption spectrum of PDPSe NPs in water, and (D) its corresponding absorption spectrum in chloroform. To make sure the same concentration of PDPSe molecules in (C) and (D), the aqueous solution used in (C) was lyophilized followed by drying in vacuum oven. The obtained powder was re-dissolved in chloroform with the same concentration in (C), which was used to measure the corresponding absorption

spectrum (D). According to the absorption intensity at 808 nm in (D) and the mass extinction coefficient of PDPSe in chloroform, we can calculate the actual concentration of PDPSe molecules in (C) and (D). Based on (C) and the obtained actual concentration of PDPSe molecules, the mass extinction coefficient of PDPSe NPs in water was determined to be 44.9 L g^{-1} cm^{-1}.

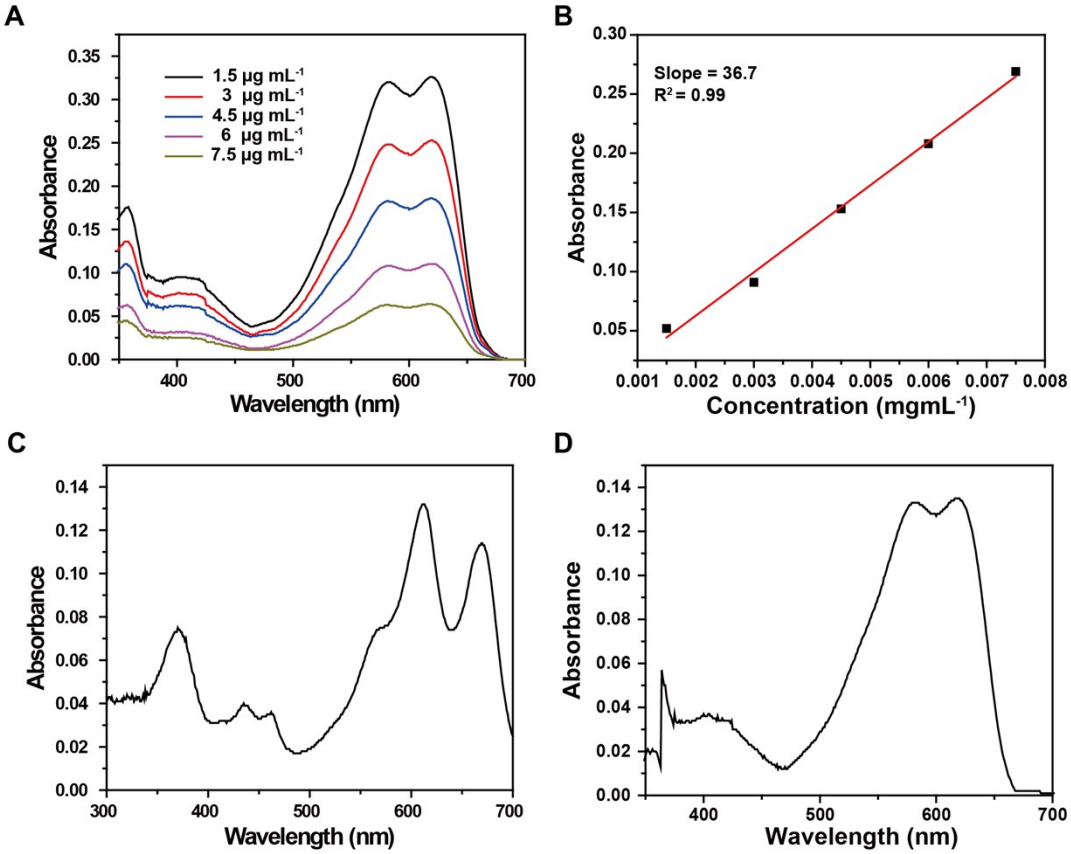

Fig. S8 Measurement of the mass extinction coefficient of DPSe NPs in water. (A) Absorption spectra of DPSe in chloroform with different concentrations. (B) Optical density of DPSe at 635 nm plotted as a function of concentration of DPSe in chloroform. The slope was used to determine the mass extinction coefficient (36.7 L g^{-1} cm^{-1}). (C) Absorption spectrum of DPSe NPs in water, and (D) its corresponding

absorption spectrum in chloroform. To make sure the same concentration of DPSe molecules in (C) and (D), the aqueous solution used in (C) was lyophilized followed by drying in vacuum oven. The obtained powder was re-dissolved in chloroform with the same concentration in (C), which was used to measure the corresponding absorption spectrum (D). According to the absorption intensity at 635 nm in (D) and the mass extinction coefficient of DPSe in chloroform, we can calculate the actual concentration of DPSe molecules in (C) and (D). Based on (C) and the obtained actual concentration of DPSe molecules, the mass extinction coefficient of DPSe NPs in water was determined to be 26.2 L g^{-1} cm^{-1}.

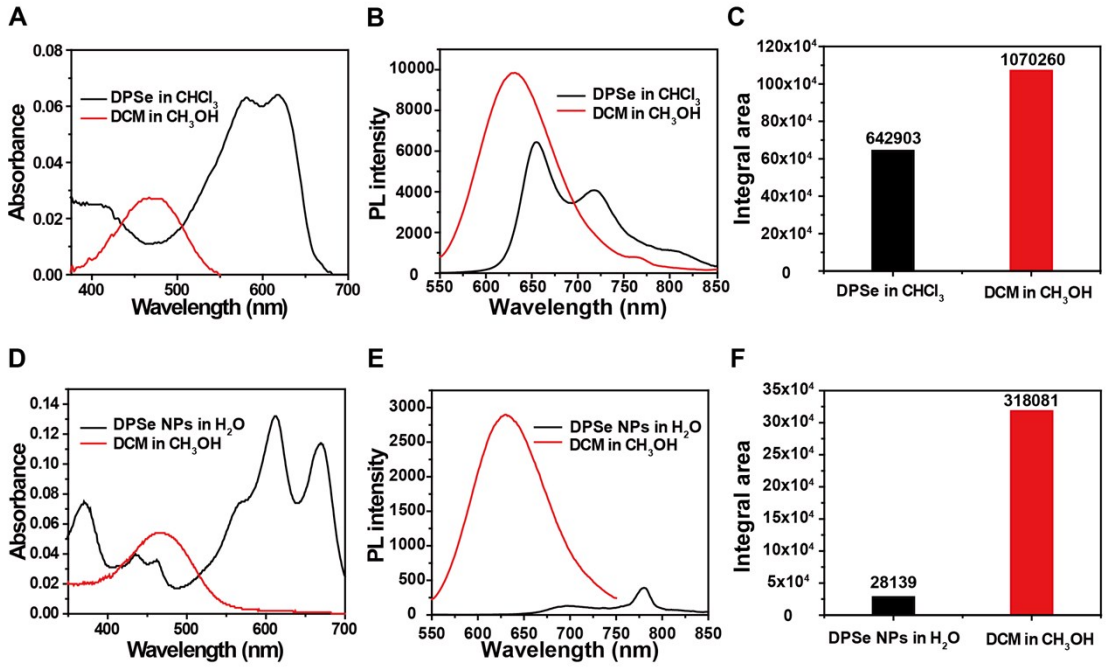

Fig. S9 QY measurement of DPSe in chloroform and DPSe NPs in water. (A) UV-vis-NIR absorption and (B) PL spectra of DCM in methanol and DPSe in chloroform. The PL spectra were obtained under an excitation at 505 nm. (C) Integral area of the PL spectra in (B). The QY of DPSe in chloroform was calculated to be 30.6%. (D) UV-

vis-NIR absorption and (E) PL spectra of DCM in methanol and DPSe NPs in water. The PL spectra were obtained under an excitation at 515 nm. (F) Integral area of the PL spectra in (E). The QY of DPSe NPs in water was calculated to be 3.8%.

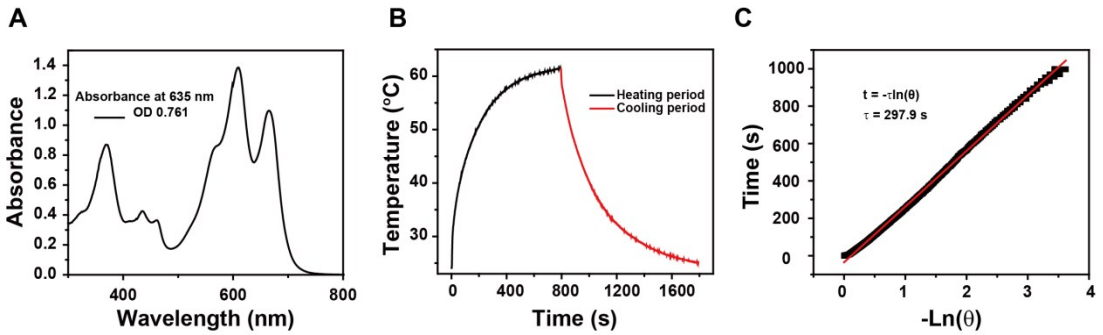

Fig. S10 PCE measurement of DPSe NPs in water. (A) Absorption spectrum of DPSe NPs in water. (B) Photothermal effect of DPSe NPs under irradiation of a 635 nm laser (1 W cm^{-2}), which was turned off after irradiation for 800 s. (C) Plot of cooling time versus negative natural logarithm of the temperature driving force obtained from the cooling stage shown in (B). PCE of DPSe NPs is calculated to be 40%.

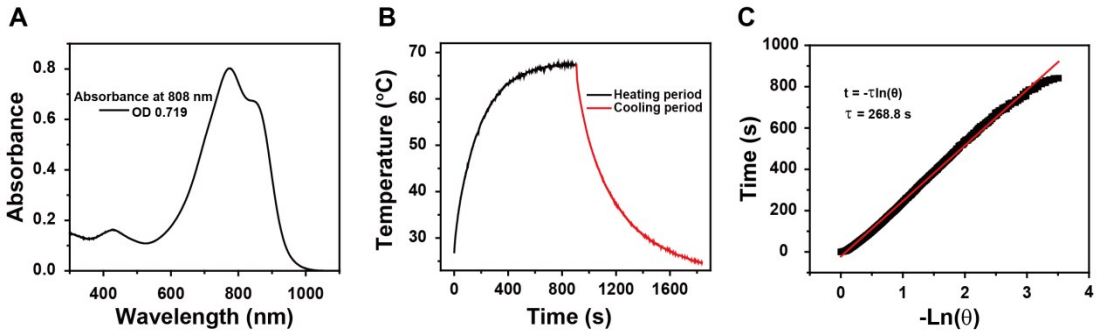

Fig. S11 PCE measurement of PDPSe NPs in water. (A) Absorption spectrum of PDPSe NPs in water. (B) Photothermal effect of PDPSe NPs under irradiation of an 808 nm laser (1 W cm^{-2}), which was turned off after irradiation for 850 s. (C) Plot of cooling

time versus negative natural logarithm of the temperature driving force obtained from the cooling stage shown in (B). PCE of PDPSe NPs is calculated to be 62.5%.

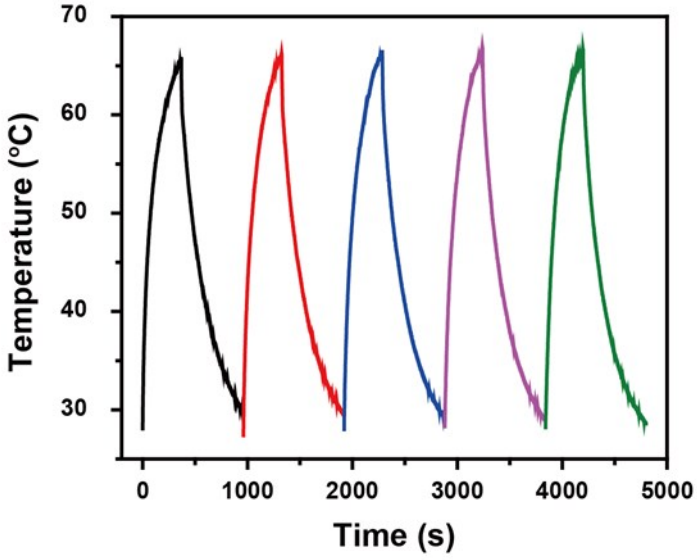

Fig. S12 Temperature changes of PDPSe NPs at a concentration of 75 μg mL^{-1} over five laser ON/OFF cycles of 808 nm laser irradiation.

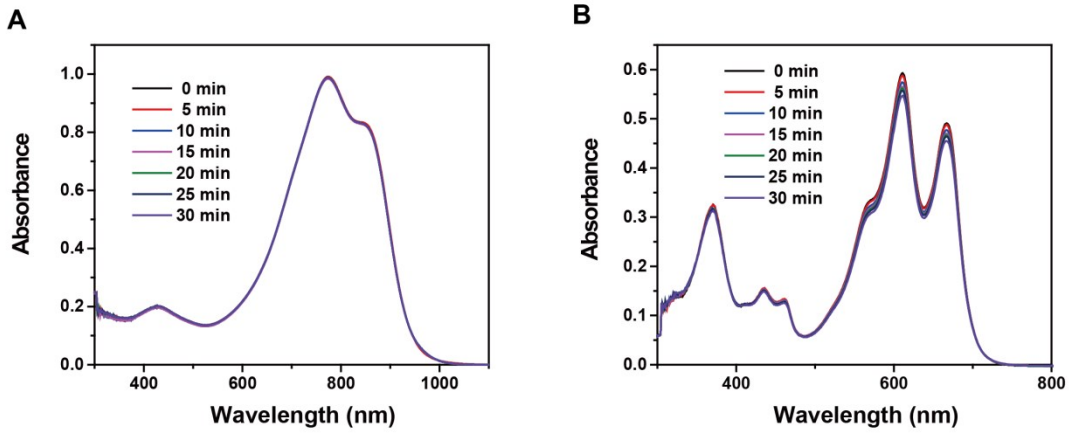

Fig. S13 Photostability measurement of PDPSe NPs and DPSe NPs. Absorption spectra of PDPSe NPs (A) and DPSe NPs (B) after exposure to a 635 nm laser irradiation (1.5 W cm^{-2}) for 30 minutes.

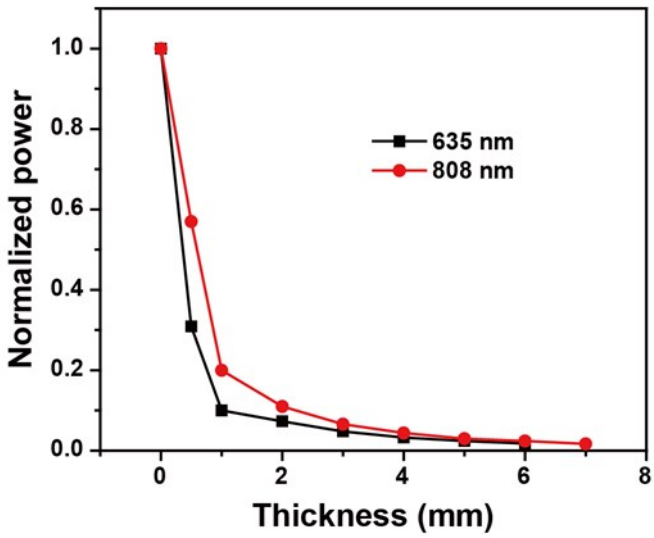

Fig. S14 Normalized excitation laser power versus depth of phantom composed of 1% intralipid under excitation at 635 nm and 808 nm.

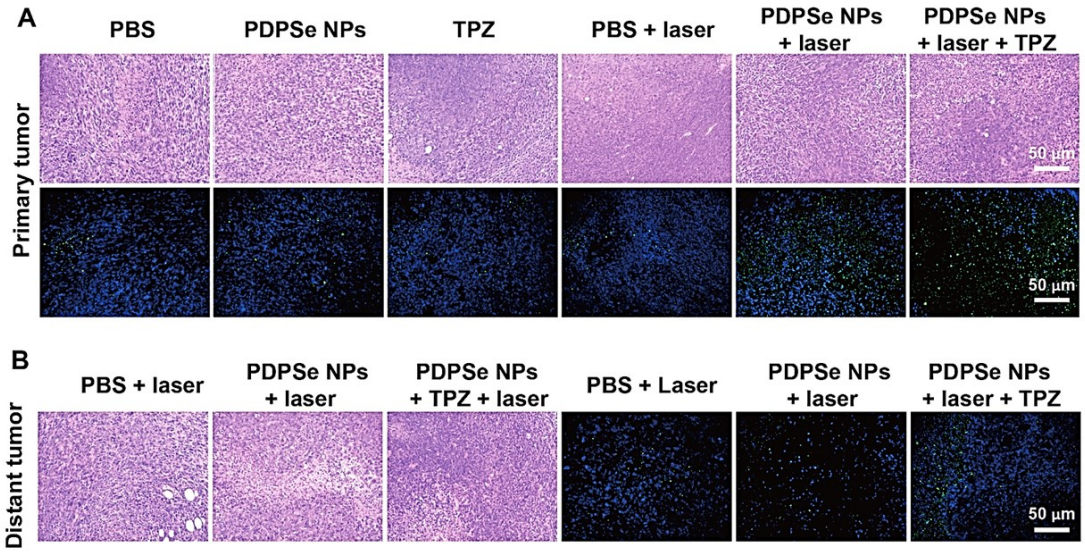

Fig. S15 H&E and TUNEL-stained images of the primary tumors (A) and distant tumors (B) excised at day 24 after different treatments.

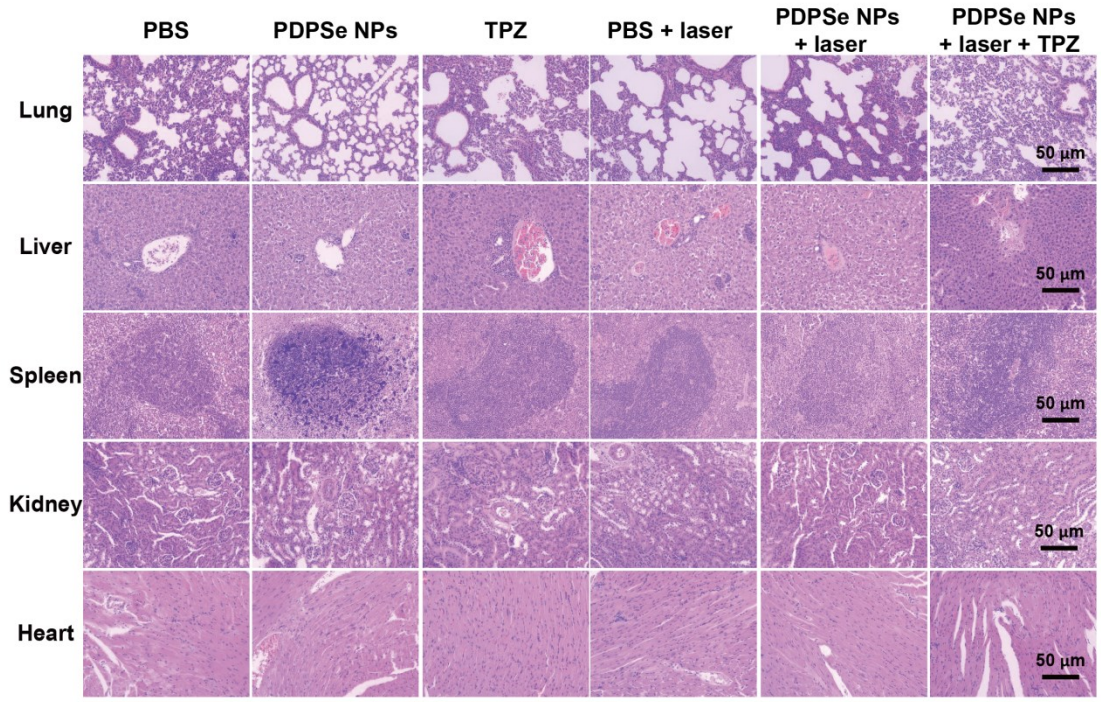

Fig. S16 H&E staining of important organs (lung, liver, spleen, kidney and heart).

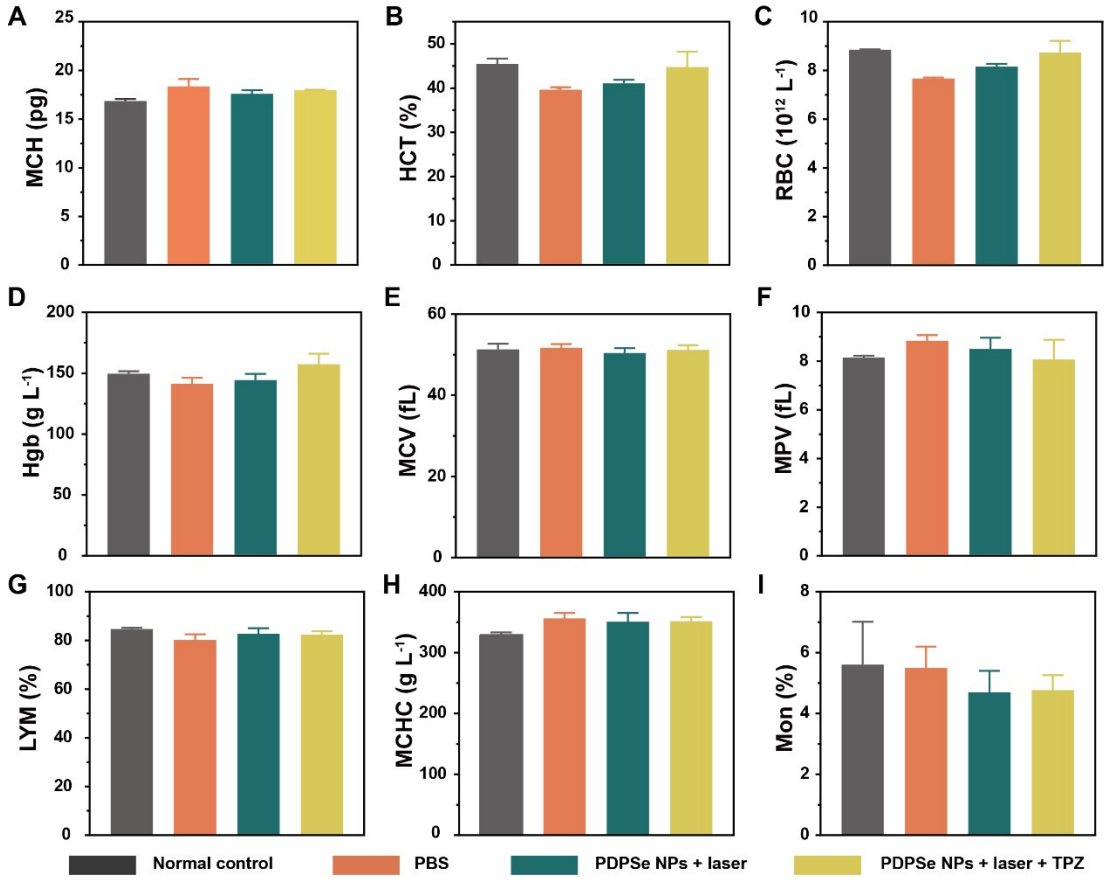

Fig. S17 Serum biochemistry of mice treated with PDPSe NPs. (A) Mean corpuscular hemoglobin (MCH). (B) Hematocrit (HCT). (C) Red blood cell (RBC). (D) Hemoglobin (Hgb). (E) Mean corpuscular volume (MCV). (F) mean platelet volume (MPV). (G) Lymphocytes LYM). (H) Mean corpuscular hemoglobin concentration (MCHC). (I) Monocytes (Mon).

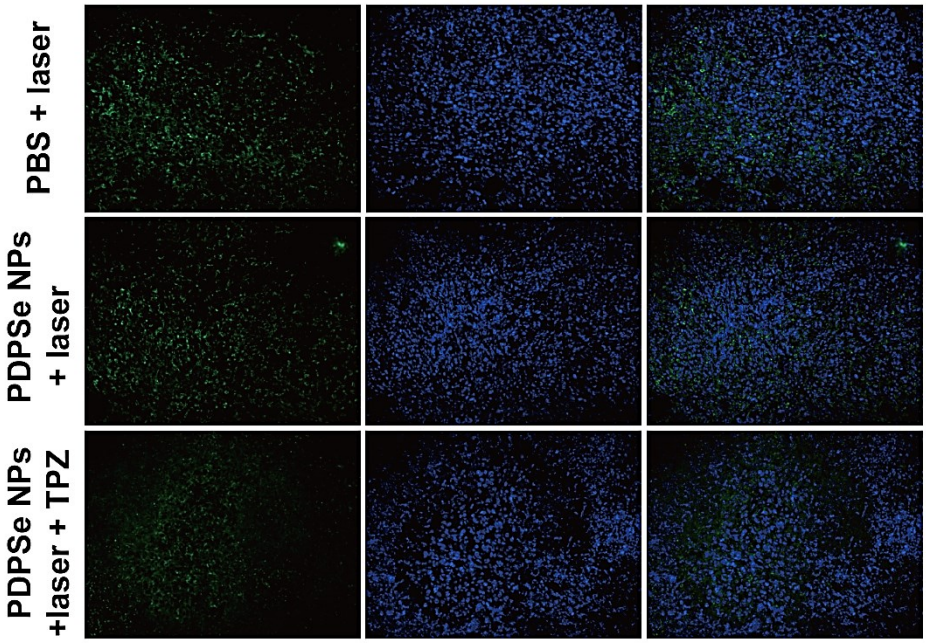

Fig. S18 Immunofluorescence images of HIF-α on day 24 after different treatments on the primary tumors.

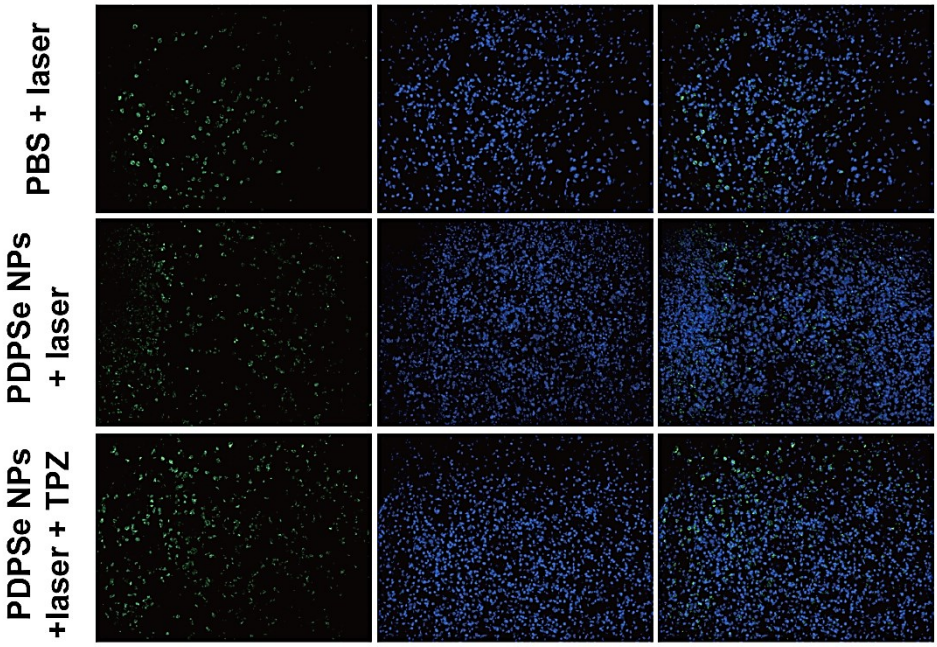

Fig. S19 M1 macrophage in the primary tumors on day 24 after different treatments on the primary tumors.

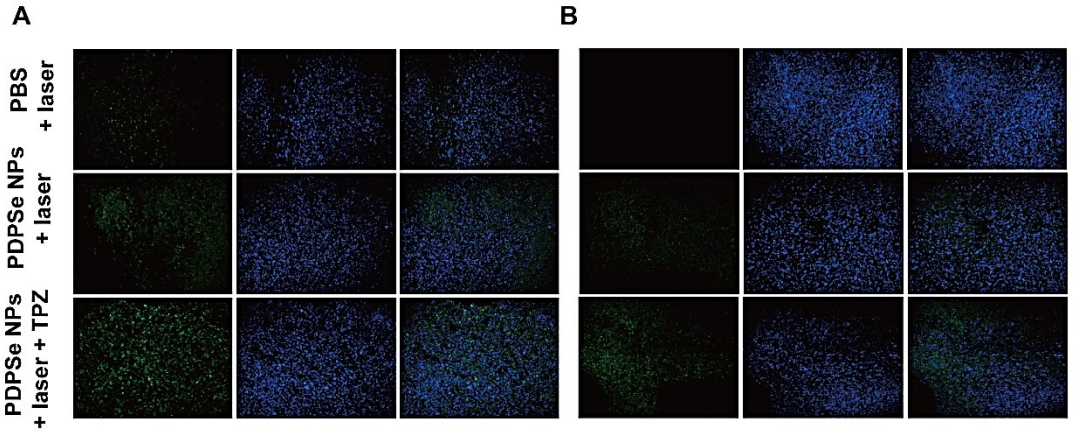

Fig. S20 Immunofluorescence images of effector CD8+ T cells in primary tumors (A) and distant tumors (B) on day 24 after different treatments on the primary tumors. The tumor tissue slices were immune-stained with anti-CD8-FITC (green).

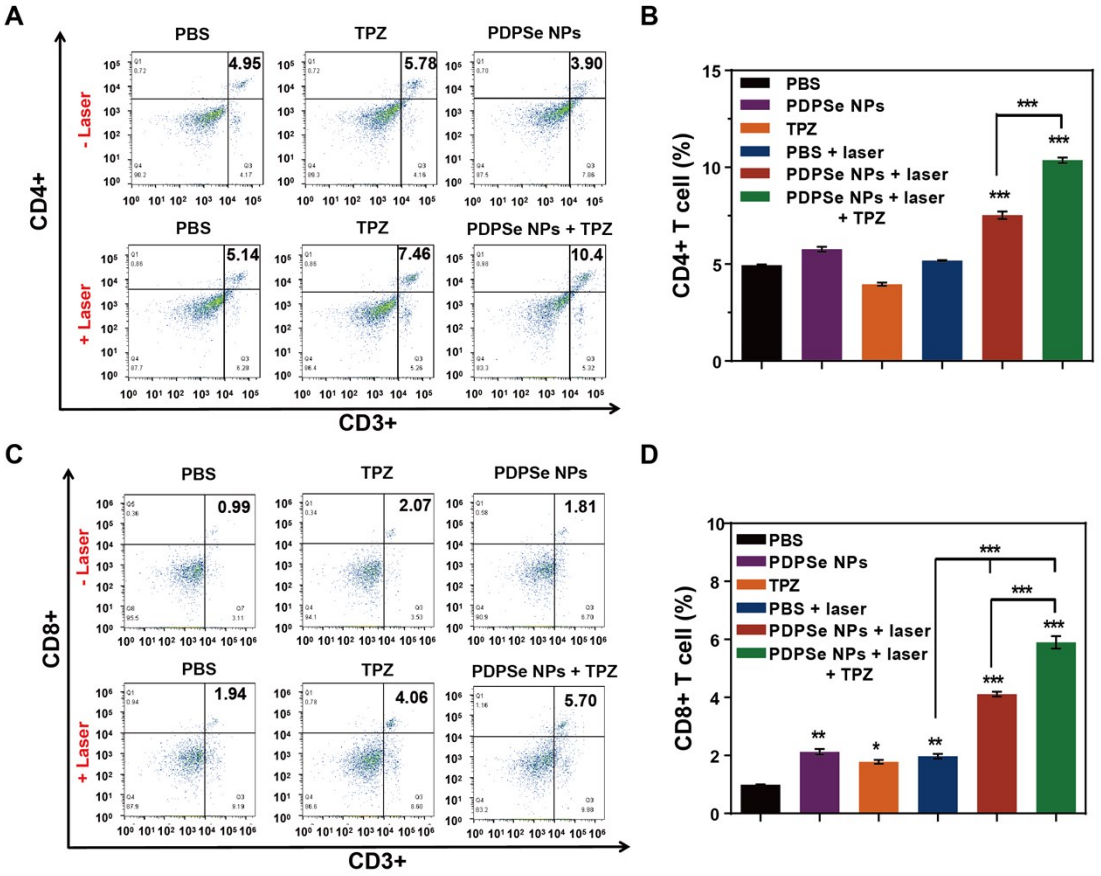

Fig. S21 (A) Flow cytometry analysis of CD4+ cells on day 12 after different treatments for the primary tumor after different treatments for the primary tumor. (B) Proportion of tumor infiltrating CD4+ cells based on (A). (C) Flow cytometry analysis of CD8+ cells on day 14 after different treatments for the primary tumor. (D) Proportion of tumor infiltrating CD8+ cells based on (C).

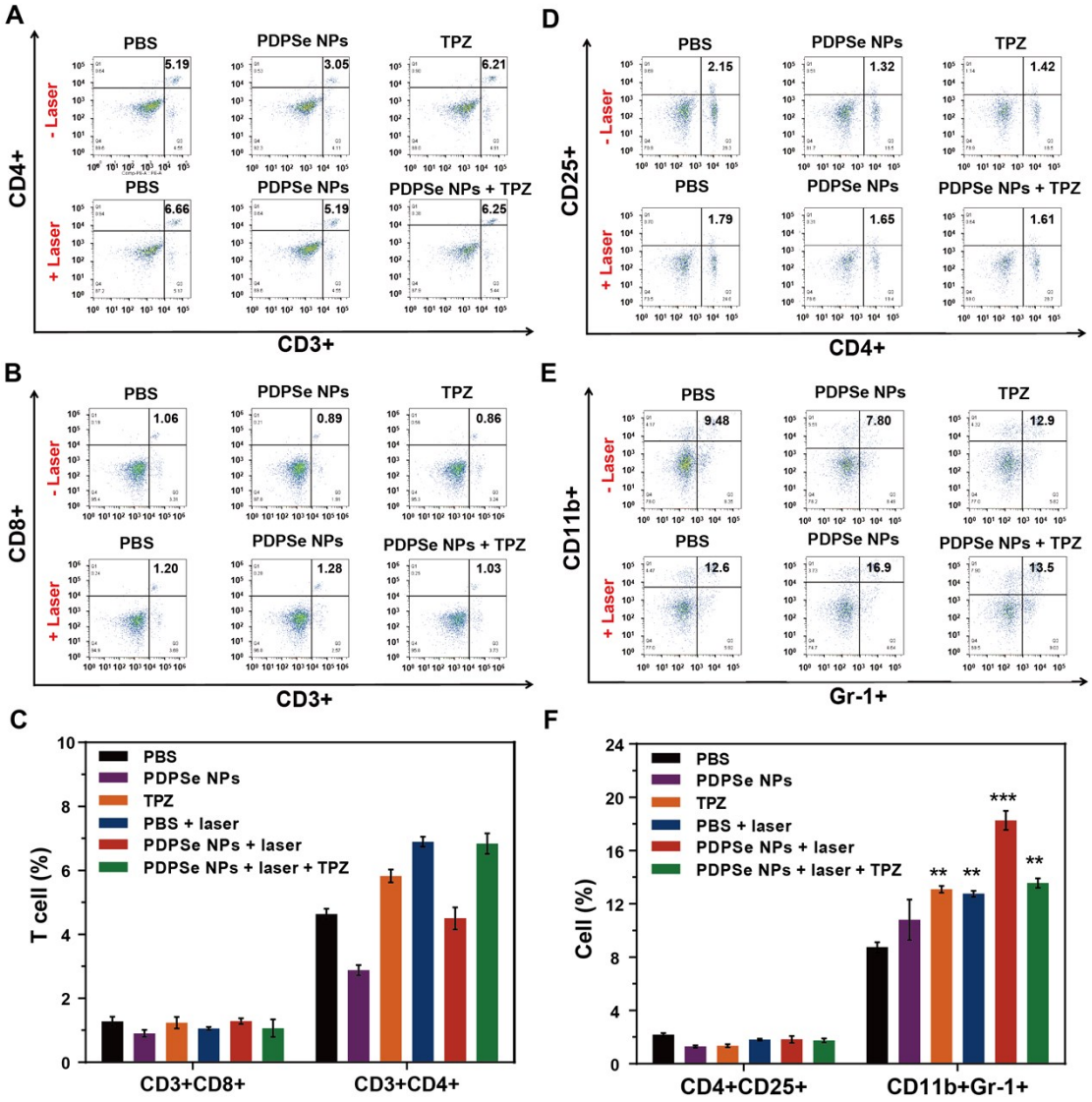

Fig. S22 Flow cytometry of T cells and myeloid-derived suppressor cells in spleen cells. Flow cytometry of CD4+ cells in CD3+ T cells (A) and CD8+ in CD3+ T cells (B). (C) Proportion of tumor infiltrating CD8+ cells and CD4+ cells based on (A) and (B). Flow cytometry of CD25+ cells in CD4+ T cells (D) and MDSCs after different treatments on day 17. (F) Proportion of tumor infiltrating CD25+ cells and MDSCs based on (D) and (E).